Agronomy Journal, pp. 235-244, Vol. 87, No. 2, 1995.

Measured and Simulated Surface Soil Drying

Abdu A. Durar,* Jean L. Steiner, Steven R. Evett, and Edward L. Skidmore

ABSTRACT

The USDA initiated the Wind Erosion Prediction System (WEPS) to develop improved technology for predicting wind erosion. A HYDROLOGY submodel has been developed for WEPS to simulate the soil energy and water balances. This study was conducted to evaluate the performance of the HYDROLOGY submodel in predicting surface soil drying. Water content was measured gravimetrically in a bare 5- by 30-m plot for 14 d after irrigation during July and August 1991. The plot was located 5 m directly north of a bare weighing lysimeter at the USDA-ARS Conservation and Production Research Laboratory at Bushland, TX. Hourly samples were taken from depth increments of 0 to 2, 2 to 6, 6 to 10, 10 to 30, and 30 to 50 mm. Furthermore, soil cores were taken to 900 mm at 6-h intervals. Water content was also measured daily at the lysimeter and between the lysimeter and gravimetric sampling plot using a neutron probe to 2.1 m. The submodel accurately predicted that no deep percolation occurred throughout the simulation period. Simulation results agreed well with the measured daily evaporation rates from the lysimeter (r^2 = 0.96). Furthermore, the submodel reasonably estimated the soil water content profiles, particularly the status of soil water at the soil–atmosphere interface. The mean absolute error, which describes the average absolute deviation between measured and simulated soil water contents, was 0.015 m^3 m^{-3}. The HYDROLOGY submodel of WEPS shows a potential to accurately simulate soil water dynamics, as needed for wind erosion modeling. The submodel successfully predicts the changes in water content at the soil surface, which relate to the susceptibility of the soil to wind erosion.

THE STATUS OF SOIL WATER, particularly in the surface layer, plays an important role in the management of our soil resources (Skidmore, 1979). For example, the soil water content in the uppermost few millimeters of the soil significantly influences the susceptibility of the soil to wind erosion. Chepil (1956) and Bisal and Hsieh (1966) conducted independent wind-tunnel experiments to study soil erodibility by wind as influenced by water content of the soil surface. They concluded that most soils are resistant to wind erosion when the water content of the soil surface is above that retained at -1.5 kJ kg^{-1} soil matric potential (i.e., when the soil surface is wetter than the wilting point).

Significant drying of the soil surface usually occurs when the evaporation rate from the surface layer exceeds the rate of water movement toward the surface from the underlying soil layers. Several scientists (Jackson, 1973; Reginato, 1975; Idso et al., 1975) conducted field experiments at Phoenix, AZ, to investigate the influences of bare soil evaporation on the status of soil water in the uppermost few millimeters of an Avondale loam [fine-loamy, mixed (calcareous), hyperthermic Typic Torrifluvent]. Reginato (1975) measured soil water content gravimetrically in the uppermost 1-mm layer using samples taken every 20 min during 1 d of soil drying in February. He found that the water content decreased from 0.202 to 0.036 m^3 m^{-3} in the 8 h between 0800 and 1600 h. Idso et al. (1975) used albedo measurements to estimate water content of the soil surface. They found that the water content decreased from 0.20 to 0.07 m^3 m^{-3} between 1300 and 1500 h on the second day after the soil was irrigated in July. Jackson (1973) found that 5 d after the soil was irrigated in March, the water content in the uppermost 5 mm decreased from 0.235 m^3 m^{-3} at sunrise to 0.097 m^3 m^{-3} at 1500 h. However, the water content increased at night and reached a maximum of $\approx$0.19 m^3 m^{-3} at 0600 h on the next day, then decreased rapidly again during the day to a new minimum of 0.065 m^3 m^{-3} at 1700 h.

This trend of the surface layer to dry during the day and to partially rewet at night was evident for every measurement day, including the 37th and final day of the experiment. The findings of these researchers (Jackson, 1973; Reginato, 1975; Idso et al., 1975) are significant, considering that the field capacity and wilting point of the Avondale loam are 0.255 and 0.146 m^3 m^{-3}, respectively (Brust et al., 1968; Jackson, 1964). This implies that, when the ambient climatic conditions were particularly conducive to soil drying, water content of the soil surface of the Avondale loam decreased from very wet to sufficiently dry to be susceptible to wind erosion in only a few hours. The drying of the soil surface can occur more rapidly in coarse-textured soils. Skidmore and Dahl (1978) used a modified version of Hillel's (1977) model for nonisothermal soil evaporation to simulate soil-water dynamics for the uppermost 10 mm of the soil as influenced by climatic conditions, soil hydraulic properties, and initial water content. Hourly meteorological parameters were used to calculate soil evaporation from three soils with a clay, loam, or sand texture. The uppermost 10 mm of the three soils dried quickly to the critical level for erodibility by wind, particularly when the meteorological conditions were conducive to wind erosion. When the soil was initially wet and weather was dominated by medium to high radiation and strong winds, the soils with sand, loam, and clay textures dried to the threshold of erodibility by wind by the first, second, and third day, respectively.

Mech (1955) observed that evaporation quickly depletes the water content of the soil surface, especially in the arid and semiarid regions of the world. Although the depth of dryness may be only the uppermost few millimeters and the soil below may be wet, if the wind attains the threshold velocity required to initiate soil movement, the dry surface layer can erode easily unless the surface soil particles are clustered into nonerodible aggregates or the soil surface is protected by vegetation. Troeh et al. (1980) reported that, in some sandy soils when the climatic conditions are conducive to rapid drying of the surface soil,

A.A. Durar and E.L. Skidmore, USDA-ARS Wind Erosion Res. Unit, Throckmorton Hall, Kansas State Univ., Manhattan, KS 66506; J.L. Steiner, USDA-ARS Southern Piedmont Conservation Res. Ctr., P.O. Box 555, Watkinsville, GA 30677; and S.R. Evett, USDA-ARS Conservation & Production Res. Lab., P.O. Drawer 10, Bushland, TX 79012. Contribution from the USDA-ARS in cooperation with the Kansas Agric. Exp. Stn. Contribution no. 93-157-J. Received 7 June 1993. *Corresponding author (Email: durar@weru.ksu.edu).

Published in Agron. J. 87:235–244 (1995).

Abbreviations: DOY, day of year; MAE, mean absolute error.

wind erosion can begin within 15 to 20 min after an intense shower.

THE WIND EROSION PREDICTION SYSTEM (WEPS) PROJECT

The USDA initiated the Wind Erosion Prediction System (WEPS) project to develop improved technology to predict wind erosion (Hagen, 1991). The structure of WEPS is modular, consisting of a MAIN (supervisory) program, a user-interface input section, an output control section, and seven submodels (WEATHER, SOIL, HYDROLOGY, CROP, DECOMPOSITION, MANAGEMENT, and EROSION) along with their associated data bases (Fig. 1).

An accurate evaluation of soil water content is a prerequisite for any reliable wind erosion prediction scheme. Therefore, a computer simulation of soil-water dynamics has been developed for the HYDROLOGY submodel of WEPS to simulate the soil energy and water balances (Durar, 1991). Some of the algorithms used in the HYDROLOGY submodel are similar to those used in well-established watershed models such as SPAW (Saxton and Bluhm, 1982; Saxton et al., 1974; Sudar et al., 1981), CREAMS (Smith and Williams, 1980), and EPIC (Williams et al., 1984, 1990). Significant modifications were made, however, and new algorithms were added to meet the unique requirement of WEPS for fast simulation of the diurnal changes in soil water content, particularly at the soil–atmosphere interface (Durar, 1991).

The HYDROLOGY Submodel of WEPS

The HYDROLOGY submodel of WEPS provides a simplified representation of the complex processes and interactions that govern soil-water dynamics. These simplifications were necessary to meet the requirements of WEPS for fast simulation of the soil water and energy balances using daily weather and readily available soil data as inputs. The user requirement document of the WEPS project specifies that WEPS should simulate wind erosion from a homogeneous simulation region at the rate of 2 min of computation time for each year of the crop rotation. For all practical purposes, the time restriction eliminates any complex and consequently time-consuming simulation of soil-water dynamics that takes into account multidimensional and/or nonisothermal conditions. In comparison, mechanistic research models such as ENWATBAL (Evett and Lascano, 1993) are usually based on numerical solutions of the coupled soil water and heat flow equations. The HYDROLOGY submodel of WEPS maintains a continuous soil-water balance by accounting for daily amounts of snow melt, runoff, infiltration, deep percolation, soil evaporation, and plant transpiration.

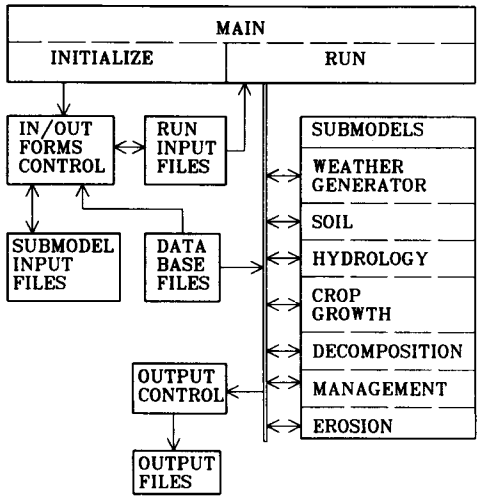

Fig. 1. Schematic of the Wind Erosion Prediction System (WEPS).

The snow melt component of the submodel is similar to that of the CREAMS model (Smith and Williams, 1980) and the EPIC model (Williams et al., 1984; 1990). If snow is present on any given day, it begins to melt when the maximum daily air temperature exceeds 0°C. The daily amount of snow melt depends on the maximum air temperature of that day and the initial water content of the snow. Snow melt is added to the water available for infiltration and runoff. If measured runoff amount is not available as a data input, the runoff is calculated using a modified version of the Soil Conservation Service (SCS) curve number method (Soil Conservation Service, 1972).

The daily total amount of water available for infiltration is the sum of the rainfall, irrigation, and/or snow melt amounts minus the runoff amount. The water available for infiltration is stored in the soil profile from the top down. Water is added to the uppermost simulation layer until its water content reaches field capacity, then any excess water is cascaded downward to succeeding layers. Each layer is filled to field capacity before the next layer is assigned any water. This proceeds until the available water is used up or the lowermost simulation layer is filled to field capacity at which point any remaining water is assigned to deep percolation.

Potential evapotranspiration is calculated using a revised version of Penman's combination method (Van Bavel, 1966). The total daily potential evapotranspiration (ET_p) is then partitioned on the basis of the leaf area index of the crop into potential soil evaporation (E_p) and potential plant transpiration (T_p). The daily potential soil evaporation (E_p) is partitioned to obtain hourly estimates of potential soil evaporation (E_{ph}) using a sine function similar to that used by Hillel (1977). The hourly estimates of actual soil evaporation (E_{ah}) are obtained by adjusting the hourly potential rates on the basis of soil water availability.

Furthermore, the submodel simulates soil water redistribution using Darcy's law and a simplified finite difference approach similar to that used by Hillel (1977). The submodel redistributes soil water in the soil profile on an hourly basis assuming isothermal and one-dimensional water flow conditions. Soil water flux between any two of the n layers of a finite difference representation of the soil profile is controlled by the water potential gradient between those two layers and by the average hydraulic conductivity of the two layers. The relatively simple method of Campbell (1974) is used to calculate the unsaturated hydraulic conductivity as a function of volumetric water content, θ (m^{-3} m^{-3}). This method assumes that the soil water characteristic curve can be represented by

$$\psi = \psi_e \, (\theta/\theta_s)^{-b} \qquad [1]$$

where ψ is the matric potential (J kg^{-1}), ψ_e is the air entry potential (J kg^{-1}), θ_s is the saturated water content (m^3 m^{-3}), and b is a constant defined as the inverse of the pore size distribution index. The unsaturated hydraulic conductivity, K (m s^{-1}), is represented by

$$K = K_s \, (\theta/\theta_s)^{2b+3} \qquad [2]$$

where K_s is the saturated hydraulic conductivity (m s^{-1}).

The standard approach in simulating the water content at the soil–atmosphere interface is to set the depth of the uppermost simulation layer to a few millimeters and consider that layer as the upper boundary condition of the governing water flow equations. The drawback of this approach is the increase in computation time, which limits its use to research models. As described by Durar (1991), the HYDROLOGY submodel allows the uppermost simulation layer to be relatively thick (50 mm), to speed the computation time. The submodel, however, provides

hourly estimates of water content at the soil–atmosphere interface by extrapolating water content to the soil surface from the three uppermost simulation layers and by interpolating the relationship between water content of the soil surface and the ratio of actual to potential evaporation. The combination of the extrapolation and interpolation schemes was developed by Durar (1991) on the basis of the data collected by Jackson (1973). Accordingly, soil water content at the soil–atmosphere interface is estimated by using the equations

$$\theta_0 = \text{AMIN1}\ (\theta_{er}, \theta_x, \theta_{0i}) \quad E_{ph} > 0.0,\ \text{PRCP} = 0 \quad [3]$$

$$\theta_0 = \text{AMAX1}\ (\theta_x, \theta_{0i}) \quad E_{ph} = 0.0,\ \text{PRCP} = 0 \quad [4]$$

$$\theta_0 = \theta_x \quad \text{PRCP} > 0 \quad [5]$$

where θ_0 is the soil water content at the soil–atmosphere interface ($m^3\ m^{-3}$), θ_{0i} is the soil water content at the soil–atmosphere interface from the previous time increment ($m^3\ m^{-3}$), θ_x is the extrapolated water content at the soil surface ($m^3\ m^{-3}$), θ_{er} is the soil water content based on the ratio of actual to potential evaporation ($m^3\ m^{-3}$), E_{ph} is the hourly potential rate of soil evaporation (mm h^{-1}), and PRCP is the daily amount of precipitation, irrigation, and/or snow melt (mm d^{-1}). The operators AMIN1 and AMAX1 return the minimum and maximum values of their arguments, respectively.

The extrapolated water content at the soil surface (θ_x) is obtained from a solution to the simultaneous equations expressing the relationship between the water contents, θ_i, of the top three simulation layers and the depth to the bottom of each layer, z_i:

$$\theta_i = \theta_x + bz_i + cz_i^2, \quad i = 1 \text{ to } 3 \quad [6]$$

Based on the data collected by Jackson (1973), the following functional relationship between equivalent water content of the soil surface and hourly evaporation ratios was developed by Durar (1991):

$$\omega = 0.24308 + \frac{1.37918}{1 + \exp\left[-\left(\frac{\text{ERATIO} - 0.44882}{0.08100}\right)\right]} \quad [7]$$

where ω is the equivalent water content defined as the ratio of volumetric soil-water content ($m^3\ m^{-3}$) to volumetric soil-water content for the same soil at -1.5 kJ kg^{-1} soil matric potential, and ERATIO is the ratio of hourly actual evaporation (E_{ah}) to hourly potential evaporation (E_{ph}).

The water content at the soil surface based on the evaporation ratio (θ_{er}) is calculated with the equation

$$\theta_{er} = \omega \times \theta_{wp} \quad [8]$$

where θ_{wp} is the water content of the soil surface at wilting point ($m^3\ m^{-3}$).

As shown from Eq. [3] to [5], the extrapolated water content at the soil surface is used as the sole indicator of water content at the soil–atmosphere interface when there is an irrigation, precipitation, and/or snow melt event.

As a first step in the validation of the submodel, its performance was evaluated by comparing its predictions with the measured soil water content and evaporation data from a 14-d field experiment conducted during March 1971 on an Avondale loam (Jackson, 1973; Jackson et al., 1973). In general, the submodel predictions compared favorably with actual measurements of daily evaporation ($r^2 = 0.99$) and soil water content measurements ($r^2 = 0.91$) throughout the experiment. Furthermore, the submodel provided good hourly estimates of soil wetness at the soil–atmosphere interface as compared with the measured water contents from the uppermost 5 mm of soil (Durar, 1991). The data from Jackson (1973) were used to develop a key algorithm in the submodel that defines the functional relationship between surface soil wetness and the ratio of actual to potential evaporation. This study was conducted to independently evaluate the performance of a stand-alone version of the HYDROLOGY submodel of WEPS in predicting surface soil drying with different soil and climatic conditions.

MATERIALS AND METHODS

Experimental Site

The field experiment was conducted during July and August 1991 on a Pullman clay loam (fine, mixed, thermic Torrertic Paleustoll). The experimental site was a 210- by 250-m field situated at the USDA-ARS Conservation and Production Research Laboratory at Bushland, TX (35°11′ N, 102°6′ W, and 1169 m above mean sea level). A lysimeter was located at the center of the 5-ha rectangular field. The northeastern lysimeter was one of four lysimeters located at the research center. The previous crop was corn, harvested in the fall of 1990. During the fallow period prior to the experiment, the field was moldboard plowed to incorporate residues and disked three times for weed control and to smooth the surface.

Climatic and Lysimeter Data

Precipitation, net radiation, reflected solar radiation, wind speed, and wet and dry bulb temperatures were measured at the lysimeter site. Wind speed and wet and dry bulb temperatures were measured at 0.5, 0.8, 1.3, and 2.2 m above the soil surface. A tipping-bucket rain gauge was used to measure precipitation. An inverted Eppley black and white pyranometer (Model 8-48) was used to measure reflected solar radiation.[1] Solar radiation, wind speed, air temperature, and dew point temperature also were measured at a weather station located ≈400 m southeast of the lysimeter. The climatic variables were measured every 6 s, averaged for output every 15 min, and recorded by a Campbell Scientific CR7X data acquisition system. The weather station was maintained at a 1760-m^2 irrigated, mowed grass plot as described by Dusek et al. (1987).

The lysimeter was 9 m^2 in surface area with a 2.3-m-deep monolithic soil core (Marek et al., 1988). Soil water evaporation was monitored by measuring mass loss from the lysimeter at 2-s intervals. The lysimeter evaporation data were integrated for output every 5 min and recorded by a Campbell Scientific CR7X data acquisition system. The lysimeter was capable of detecting mass changes equivalent to a minimum of 0.05 mm of water (Howell et al., 1987). The minimum fetch to the lysimeter from the prevailing wind direction of south to southwest was 112 m.

On Day of Year (DOY) 215 through 217, the data acquisition system at the lysimeter partially malfunctioned because of lightning strikes. In order to replace the missing data, regression relationships were developed between data collected at the weather station and data at the lysimeter during days for which data were available for both. The regression equations were used to estimate the missing daily mean dew point temperature and wind speed and maximum and minimum daily air temperatures. Net radiation data were not available from the weather station; therefore, the missing net radiation data for DOY 215 and 216 were estimated by the HYDROLOGY submodel using the method proposed by Wright (1982). As outlined by Allen et al. (1989), the method estimates daily values of net radiation from solar radiation, air temperature, vapor pressure, and soil albedo.

[1] Mention of any trade name or product in this paper does not constitute a recommendation or endorsement for use by the USDA, nor does it imply registration under FIFRA as amended.

Irrigation and Soil Sampling

The bare field was thoroughly irrigated with ≈50 mm of water using a lateral-move sprinkler system with drop spray nozzles. Additional information about the irrigation system was given by Schneider and Howell (1990). Irrigation was started at 0700 h on 30 July and completed at 0200 h on 31 July (DOY 211 and 212 of 1991, respectively). (All times are standard time.) Intensive soil sampling for gravimetric determination of water content was initiated at 2300 h on 31 July (DOY 212), ≈23 h after the irrigation system passed the lysimeter and adjoining sampling plot. The original experimental plan called for continual sampling for a single 14-d drying cycle; however, four rainfall events occurred during the experiment. Rainfall amounts of 18.6, 1.1, 3.4, and 25 mm were measured at the lysimeter site on 3, 4, 8, and 13 August (DOY 215, DOY 216, DOY 220, and DOY 225, respectively). Soil sampling was suspended during rainfall events, but resumed when access to the field was possible and the soil was not too wet to use the soil sampling probe. The gravimetric soil sampling was terminated at 1600 h on 14 August (DOY 226).

Gravimetric soil sampling was conducted in a 5- by 30-m plot located 5 m directly north of the lysimeter. The sampling plot was divided into three subplots, each 1.7 by 30 m. During the months of June and July 1991, before the start of the experiment, the plot was roto-tilled several times and raked to smooth it comparably to the hand-tilled lysimeter. Intensive soil sampling was carried out on an hourly basis when field conditions were favorable. Special soil samplers similar to the one described by Reginato (1975) were used in this experiment to obtain samples from the 0- to 2-mm, 2- to 6-mm, 6- to 10-mm, 10- to 30-mm, and 30- to 50-mm depth increments. A regular AMS bucket auger (Art's Manufacturing & Supply, American Falls, ID), 82.5 mm in diameter, was used to make 90-mm deep access holes at each sampling time. The thin-layer soil samplers were then inserted horizontally into the sides of the hole dug by the auger to collect the soil samples.

A 25-mm diam. subsoil probe (model JMC Environmentalist's, Clements Associates, Newton, IA) was used every 6 h to collect undisturbed soil cores to 900-mm depth. The cores were sectioned into depth increments of 0 to 10, 10 to 30, 30 to 50, 50 to 70, 70 to 90, 90 to 110, 110 to 140, 140 to 160, 160 to 190, 190 to 210, 210 to 290, 290 to 310, 310 to 500, and 500 to 900 mm.

At each gravimetric sampling time, a composite sample for each depth increment was obtained by mixing the soil samples taken from the three subplots located within the 5- by 30-m sampling plot. The composited soil samples were placed into metal moisture cans with tight-fitting lids, weighed, oven-dried (at 105°C for 24 h), and then reweighed for gravimetric measurement of soil water content.

Gravimetric water contents were converted to a volumetric basis by multiplying by the average bulk density of the depth increment. Undisturbed soil cores were collected from the sampling plot to a depth of 350 mm in roughly 50-mm intervals for bulk density determination immediately after termination of gravimetric soil sampling. The bulk densities used for the uppermost 350 mm were the averages of nine core samples (three from each subplot) for each depth increment. For depth increments below 350 mm, however, bulk densities were measured at the plot prior to the experiment during neutron probe calibration. Generally, there was minimal variability in the bulk density measurements. The coefficients of variation for the bulk density measurements ranged between 1.5 and 11.7%. Therefore, it is safe to assume that variability of the soil water measurements was not significantly influenced by variability of bulk density within the sampling plot.

Gravimetric measurement of soil water content is prone to potential errors that may arise from sectioning of cores, weighing, and data acquisition and recording. To reduce scatter, the hourly volumetric water contents from the soil depth increments of 0 to 2, 2 to 6, 6 to 10, 10 to 30, and 30 to 50 mm were smoothed by a 1-2-3-2-1 weighted running average procedure similar to the one used by Jackson (1973) and Jackson et al. (1973). Accordingly, the average water content (θ) at a particular time (t) was obtained using the following expression:

$$\theta_t = (\theta_{t-2} + 2\theta_{t-1} + 3\theta_t + 2\theta_{t+1} + \theta_{t+2})/9 \quad [9]$$

where the subscripts $t+1$, $t+2$, $t-1$, and $t-2$ denote times separated from t by 1, 2, −1, and −2 sampling periods (hours), respectively.

There was minimal noise in the measured soil water content data. For example, the average absolute deviation between raw and smoothed soil water contents for the 0- to 2-mm layer was 0.004 $m^3\ m^{-3}$. However, the smoothing technique was useful to address a few outlier values that occurred during the predawn hours of DOY 219, probably because of human error.

Five access tubes were installed to measure volumetric water content on a daily basis using a neutron probe starting at the 0.1-m depth and continuing at 0.2-m intervals to 2.1 m. Two tubes were located on the lysimeter and the other three were situated between the lysimeter and gravimetric sampling plot. The Campbell Pacific Nuclear model 503DR moisture gauge had been previously calibrated for depths from 0.3 to 2.1 m with an r^2 of 0.96 (N = 39). A separate calibration equation with an r^2 of 0.91 (N = 7), was used for the 0.1-m depth.

Simulation Input Requirements

Simulation with the HYDROLOGY submodel of WEPS started on 1 Aug. 1991 (DOY 213) and continued for 14 d. Daily weather variables, soil hydrological and physical properties, and the initial water content profile were required as inputs in the simulation. The daily net radiation, maximum and minimum values of air temperature, dew point temperature, average wind speed, and rainfall amounts throughout the simulation period are given in Table 1.

Table 2 shows a summary of soil variables and initial values used in the simulation. The soil profile was divided into eight simulation layers: 0 to 0.05, 0.05 to 0.15, 0.15 to 0.3, 0.3 to 0.5, 0.5 to 0.9, 0.9 to 1.3, 1.3 to 1.7, and 1.7 to 2.1 m.

A typical soil profile of the Pullman clay loam at the research site usually consists of seven horizons: Ap, B21t, B22t, B31ca,

Table 1. Weather variables used as inputs in the Wind Erosion Prediction System (WEPS) HYDROLOGY submodel simulation of surface soil drying.†

Simulation day no.	Day of Year (1991)	Variables					
		RN	TMAX	TMIN	TDP	U	PRCP
		MJ m^{-2}	°C			m s^{-1}	mm
1	213	16.0	32.0	16.7	9.1	5.43	0.0
2	214	13.6	33.5	19.1	11.4	5.62	0.0
3	215	11.5‡	29.7	17.1	15.9	4.58	18.6
4	216	15.4‡	28.0	17.3	16.9	3.23	1.1
5	217	19.2	30.4	16.6	14.8	3.92	0.0
6	218	13.6	29.4	16.7	14.5	5.32	0.0
7	219	13.5	29.8	18.4	14.9	5.50	0.0
8	220	13.0	32.7	16.9	14.7	3.86	3.4
9	221	12.2	26.4	16.8	15.6	3.46	0.0
10	222	10.9	26.4	17.6	15.1	4.03	0.0
11	223	11.6	26.2	16.5	16.7	4.42	0.0
12	224	9.5	26.7	18.5	17.9	5.29	0.0
13	225	6.1	21.0	16.6	18.0	4.48	25.0
14	226	14.7	23.6	16.5	14.9	2.41	0.0

† Shown are the daily total net radiation (RN), maximum air temperature (TMAX), minimum air temperature (TMIN), dew point temperature (TDP), average windspeed (U), and amount of rainfall (PRCP).

‡ Estimated values from solar radiation, air temperature, vapor pressure, and soil albedo using Wright (1982) relationships as outlined by Allen et al. (1989)

Table 2. Summary of soil variables and initial values used in the Wind Erosion Prediction System (WEPS) HYDROLOGY submodel simulation of surface soil drying.†

Soil layer no.	Depth	Initial water content	Saturated water content	Field capacity	Wilting point	Water retention curve constant (b)‡	Air entry potential‡	Saturated hydraulic conductivity
	m	$m^3\ m^{-3}$					$J\ kg^{-1}$	$m\ s^{-1}$
1	0.05	0.267	0.500	0.390	0.150	7.68	−0.30	0.76×10^{-06}
2	0.15	0.284	0.500	0.390	0.150	7.68	−0.52	0.76×10^{-06}
3	0.30	0.326	0.520	0.470	0.240	9.33	−2.50	0.76×10^{-07}
4	0.50	0.348	0.520	0.470	0.240	10.09	−6.95	0.76×10^{-07}
5	0.90	0.327	0.520	0.470	0.240	9.49	−6.12	0.76×10^{-07}
6	1.30	0.317	0.520	0.470	0.240	9.26	−6.57	0.76×10^{-07}
7	1.70	0.316	0.520	0.470	0.240	9.22	−4.05	0.76×10^{-07}
8	2.10	0.291	0.520	0.470	0.240	9.22	−3.37	0.76×10^{-07}

† Sources: Taylor et al. (1963), Unger and Pringle (1981), and S.R. Evett (unpublished data).
‡ Values for water retention curve constant b and for air entry potential were estimated from particle size distribution and bulk density data as described by Campbell (1985) and modified by Flerchinger (1987).

IIB32, IIB33, and IIClca (Taylor et al., 1963). However, soil water characteristic curve and saturated hydraulic conductivity data were available for only two depth increments, 0 to 0.15 m and 0.15 to 2.10 m. Soil characteristic curves were developed from limited pressure plate data on disturbed samples. Saturated hydraulic conductivities were measured in the field using double-ring infiltrometers. The water retention curve constant (b) and the air entry potential (ψ_e) of the eight simulation layers were estimated from particle size distribution and bulk density data using the equations proposed by Campbell (1985) and modified by Flerchinger (1987).

Evaluation Criteria of Submodel Performance

The HYDROLOGY submodel of WEPS estimated soil water evaporation from the experimental site. The daily simulated evaporation rates were compared with the measured rates from the lysimeter. Furthermore, the submodel estimated soil water content of each simulation layer and at the soil–atmosphere interface. These soil water estimates were compared with the measured soil water contents. Several evaluation criteria were used to test the performance of the submodel. Data plots were used to identify the patterns of the differences between measured vs. simulated observations. However, since graphics provide only a qualitative measure of the submodel performance, quantitative performance measures were also used. Fox (1981) identified two general types of quantitative measures for the evaluation of model performance: (i) measures of correlation and (ii) measures of difference. The coefficient of determination (r^2) has been widely used as a quantitative index of correlation between measured and simulated observations. It generally describes the proportion of the total variance explained by the model. However, several scientists (Willmott, 1981, 1982; Robinson and Hubbard, 1990) have expressed strong reservations about using the coefficient of determination alone in model performance analysis. The main problem is that the magnitudes of r^2 are not consistently related to the accuracy with which the model predicts the measured data. Furthermore, the measured and simulated variables sometimes do not conform to the assumptions that are prerequisites to the application of regression analysis. Fox (1981) recommended the use of mean absolute error (MAE) as a difference measure in model performance analysis; similarly, Willmott (1981) contended that MAE is among the best overall measures of model performance. The mean absolute error, which describes the average absolute deviation between simulated and measured data, is defined as follows:

$$\text{MAE} = \frac{1}{N}\sum_{i=1}^{N} |S_i - M_i| \qquad [10]$$

where S and M are the paired simulated and measured values of the variable of interest at a given time, respectively, and N is the total number of observations.

RESULTS AND DISCUSSION

The performance of the HYDROLOGY submodel in predicting the daily soil water balance of the Pullman clay loam throughout the simulation period is summarized in Table 3. Because the soil was bare throughout the dura-

Table 3. Summary of the daily soil water balance simulation by the Wind Erosion Prediction System (WEPS) HYDROLOGY submodel.

Simulation day no.	Day of Year (1991)	Variables†						
		E_p	E_s	E_m	PERC	PRCP	RUNOFF	SWC
		mm						
–	212	–	–	–	–	–	–	660.7
1	213	11.5	4.3	4.2	0	0.0	0	656.4
2	214	11.1	1.4	2.3	0	0.0	0	655.0
3	215	6.9	1.3	1.5	0	18.6	0	672.3
4	216	6.5	5.5	5.3	0	1.1	0	667.9
5	217	9.1	4.2	4.5	0	0.0	0	663.7
6	218	8.4	2.2	2.0	0	0.0	0	661.5
7	219	8.7	1.6	1.8	0	0.0	0	659.9
8	220	7.8	1.2	1.9	0	3.4	0	662.1
9	221	5.6	2.1	2.7	0	0.0	0	660.0
10	222	5.8	1.2	1.2	0	0.0	0	658.8
11	223	5.5	0.8	0.7	0	0.0	0	658.0
12	224	5.3	0.6	0.9	0	0.0	0	657.4
13	225	2.1	2.1	2.2	0	25.0	0	680.3
14	226	5.4	4.3	4.2	0	0.0	0	676.0
Sum		99.7	32.8	35.4	0	48.1	0	

† Variables: daily potential evaporation (E_p), simulated evaporation (E_s), measured evaporation (E_m), deep percolation (PERC), amount of rainfall (PRCP), amount of runoff (RUNOFF), and soil profile water content (SWC).

tion of the experiment, the simulated potential evaporation (E_P) was equal to the simulated potential evapotranspiration (ET_P) for every simulation day. The initial soil profile water content was 660.7 mm. The final soil profile water content was 676.0 mm, indicating that a net gain of 15.3 mm of water was estimated by the end of the simulation period. A total gain of 48.1 mm of water was attributed to the four rainfall events that occurred during the experiment. A total loss of 32.8 mm of water was predicted by the submodel as a result of soil water evaporation, compared with 35.4 mm measured by the lysimeter. No significant amount of deep percolation was detected from the lysimeter and none was predicted during the simulation; therefore, the total change in the soil profile water content (SWC) was attributed exclusively to precipitation and soil water evaporation.

Comparison between Measured and Simulated Evaporation Rates

The fit between the simulated daily evaporation (E_s) and the measured daily evaporation from the lysimeter (E_m) was good throughout the experiment (Fig. 2). The MAE for daily evaporation rates over the 14 d was 0.27 mm. The simulated values of the daily evaporation rates agreed well with those measured from the lysimeter throughout the simulation period.

Regression analysis was also used to compare measured and simulated daily evaporation rates (Fig. 3). Most of the data points either fit or are closely distributed about the 1:1 line. The calculated coefficient of determination (r^2) for the best fit line ($Y = -0.322 + 1.054X$) is 0.96. Moreover, the intercept and slope of the regression equation are not significantly different from zero and unity, respectively, at the 0.05 probability level.

Comparison between Measured and Simulated Soil Water Contents

The fit between simulated and measured hourly soil water content was good for most of the simulation layers throughout the experiment (Fig. 4). The calculated coefficient of determination (r^2) for the best fit line is 0.93. Moreover, the intercept (0.001) and the slope (0.991) of the regression equation are not significantly different from zero and unity, respectively, at the 0.05 probability level. The MAEs for water content data were 0.020, 0.019, 0.012, 0.008, 0.007, 0.002, 0.001, and 0.001 $m^3\ m^{-3}$ for simulation layers 1 through 8, respectively. The MAE for soil water content for the total number of hourly observations from the eight simulation layers was 0.015 $m^3\ m^{-3}$. A significant degree of scatter in measurements of soil water content is usually expected, because of the inherent soil spatial variability and the measuring process. The standard deviations of the means of the neutron probe readings for the second through eighth simulation layers ranged between 0.001 and 0.029 $m^3\ m^{-3}$. This indicates that the errors in simulated water content values generally were within the range of standard deviations of the means of the measured values. Furthermore, the HYDROLOGY submodel of WEPS reproduced fairly well the diurnal changes in soil water content that were measured throughout the soil profile. For example, Fig. 5 depicts the measured vs. simulated hourly soil water contents for the first simulation layer (0–50 mm).

Another important test of the performance of the HYDROLOGY submodel of WEPS in simulating surface soil drying is to compare measured and simulated water content at the soil surface. Figure 6 shows that the hourly simulated soil water content at the soil–atmosphere interface exhibited the same diurnal pattern of soil drying during daytime and partial rewetting during nighttime as was observed

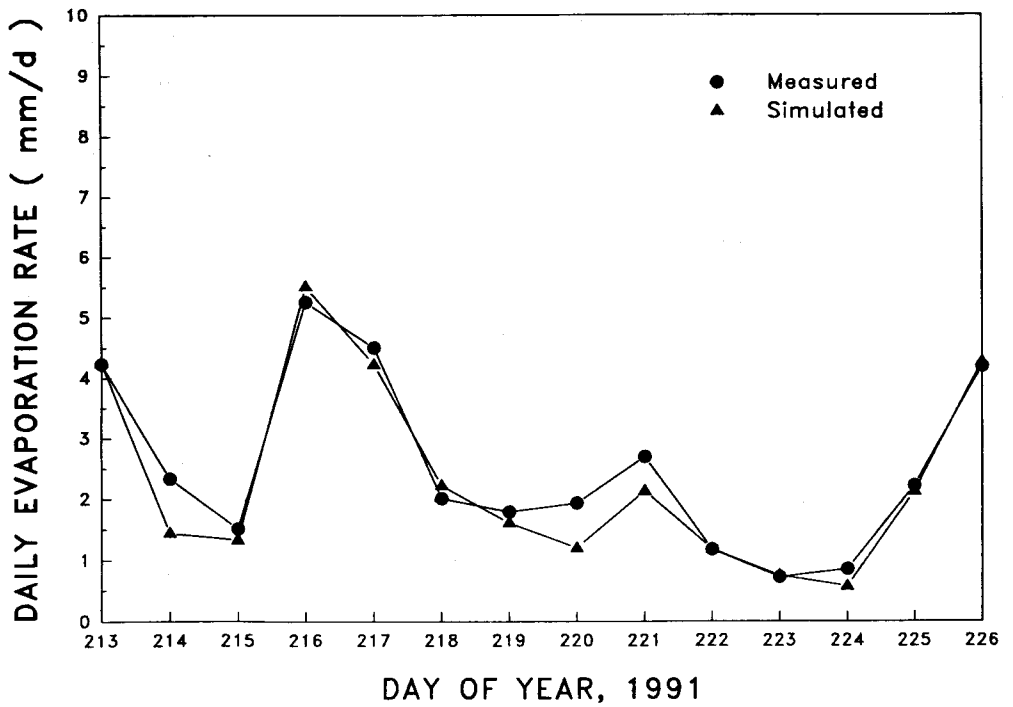

Fig. 2. Measured vs. simulated daily evaporation rates.

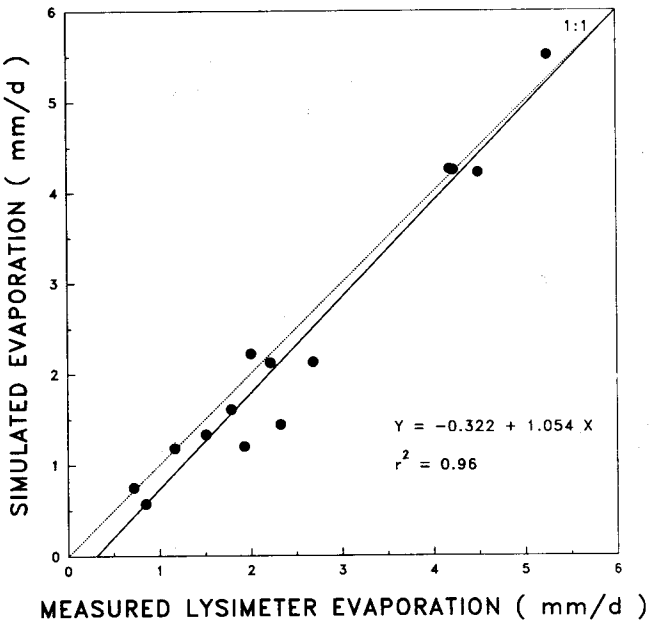

Fig. 3. Regression analysis between measured and simulated daily evaporation rates.

in the 0- to 2-mm sampling layer throughout the experiment. Furthermore, the daily amplitude of change in both simulated and measured water content at the soil surface decreased with time after irrigation or rainfall. This was particularly evident in the first three drying cycles during the first 12 d.

The MAE, which describes the average absolute deviation between simulated water content at the soil–atmosphere interface and measured water content in the uppermost 2 mm of the soil, was 0.012 m^3 m^{-3}. The most significant outcome of the simulation, however, was the ability of the submodel to accurately predict when the surface of the Pullman clay loam reached the critical level of threshold of erodibility by wind. The submodel correctly predicted that the soil was below that critical level 2 d after irrigation on the afternoon of the first day of simulation (DOY 213) and stayed in that condition for the remainder of the first drying cycle until the afternoon of the third day (DOY 215), when it rained. Furthermore, the submodel correctly predicted that water content at the soil surface remained higher than the threshold level of erodibility during the fourth day (DOY 216). However, water content dropped below the critical level on the afternoon of the fifth day (DOY 217) and remained in that condition for the remainder of the second drying cycle until the afternoon of the eighth day (DOY 220), when it rained. Water content at the soil–atmosphere interface again dropped below the critical level on the afternoon of the ninth day (DOY 221) and remained in that condition for the remainder of the third drying cycle until the early morning hours of the 13th day (DOY 225), when it rained.

Soil-Water Simulation for Wind Erosion Modeling

At 1630 h on the eighth simulation day (DOY 220), wind erosion was observed at the experimental site. Concurrently, a wind speed of 10.2 m s^{-1} was recorded 2.2 m above the lysimeter. At 1600 h, the measured water content in the uppermost 2 mm of the soil was 0.025 m^3 m^{-3}; in the

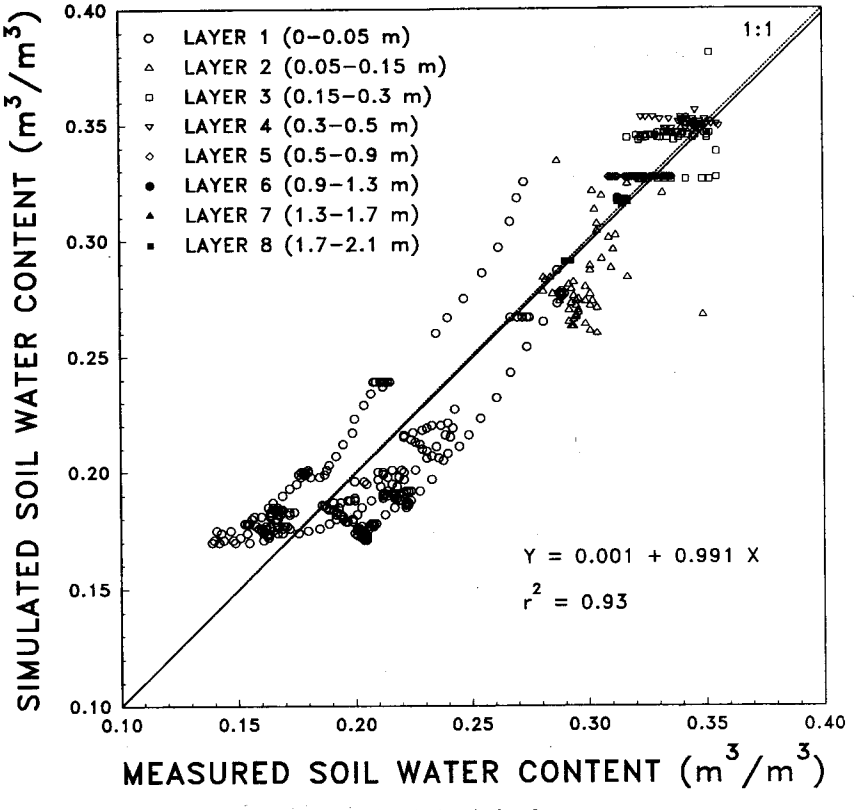

Fig. 4. Measured vs. simulated hourly soil water contents for the eight simulation layers.

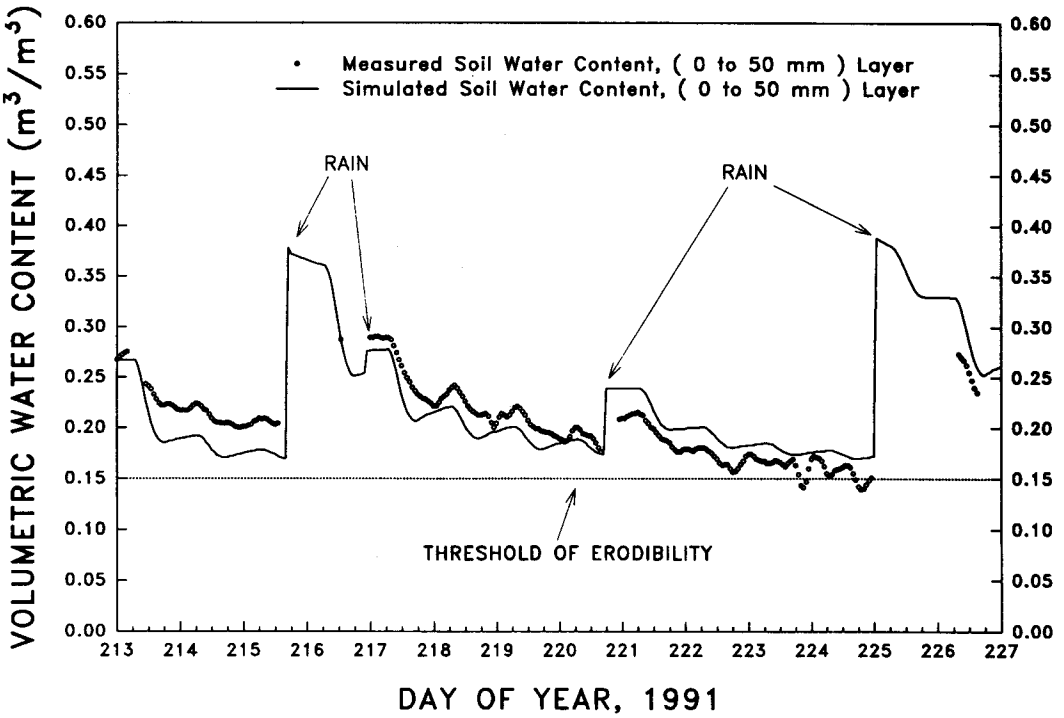

Fig. 5. Measured vs. simulated hourly soil water contents for the first simulation layer (0–50 mm).

uppermost 50 mm it was 0.176 m^3 m^{-3}. The surface of the Pullman clay loam is potentially susceptible to wind erosion when its water content is below the wilting point (i.e., when soil water content is <0.15 m^3 m^{-3}). Therefore, any assessment of the soil erodibility by wind at that point on the basis of soil water content of the entire uppermost 50 mm might lead to the wrong conclusion that the soil was not susceptible to wind erosion. This observation demonstrates that simulation of soil-water dynamics for wind erosion modeling must take into account many unique requirements, such as evaluation of soil water content at the soil–atmosphere interface. This is important, because the status of soil water content in the uppermost soil particles, which are most susceptible to wind erosion, can

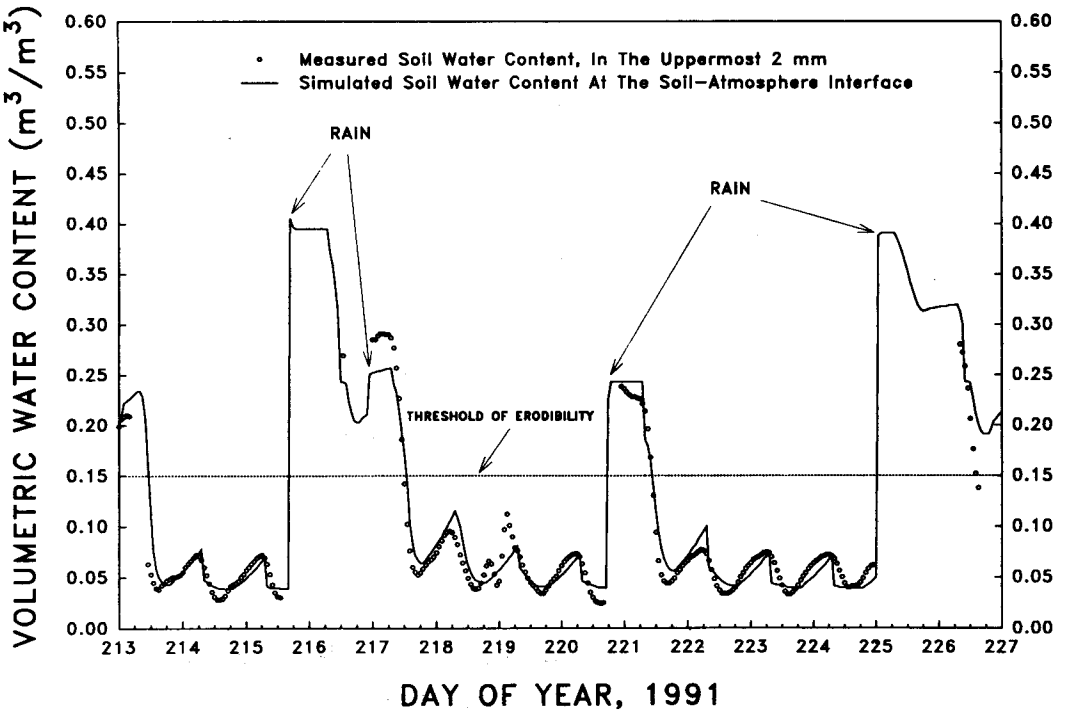

Fig. 6. Measured soil water contents in the uppermost 2 mm vs. simulated hourly soil water contents at the soil–atmosphere interface.

be significantly different from that of the subsoil. As shown in Fig. 5, the measured soil water content from the uppermost simulation layer (0–50 mm) was at or below the threshold of erodibility for only a few hours in the afternoons of the 11th (DOY 223) and 12th (DOY 224) simulation days. On the other hand, Fig. 6 shows that soil water content at the soil–atmosphere interface was significantly drier than the threshold of erodibility for most of the simulation days when no rainfall occurred. Thus, evaluating soil water content at the soil–atmosphere interface is essential to avoid any underestimation of the susceptibility of the soil to wind erosion.

Furthermore, the diurnal changes in surface soil water content (Fig. 6) demonstrate the need to predict soil water content at the soil–atmosphere interface at adequately small time steps (i.e., hourly intervals).

SUMMARY AND CONCLUSIONS

The HYDROLOGY submodel of the Wind Erosion Prediction System (WEPS) provides a highly simplified representation of the complex processes and interactions that govern soil-water dynamics. These simplifications were necessary to meet the requirements of WEPS for fast simulation of the soil water and energy balances using limited input data. The submodel's performance in evaluating surface soil drying was tested during a 14-d experiment conducted at Bushland, TX, on a Pullman clay loam. Simulation results showed good agreement between predicted and measured daily evaporation rates throughout the experiment. The closeness of fit between the predicted and measured hourly soil water contents was satisfactory for the eight simulation layers. Furthermore, the submodel provided good hourly estimates of soil water content at the soil–atmosphere interface as compared with measured water contents in the uppermost 2 mm of the soil.

The submodel successfully reproduced the dynamic changes in soil water content throughout the experiment. This occurred despite the limited quantity of some of the input data used in the simulation. Soil hydraulic properties were not available for each simulation layer.

Based on our limited testing, the HYDROLOGY submodel of WEPS shows potential for predicting the diurnal patterns of surface soil drying as needed for wind erosion modeling. The submodel also may be of interest for other applications, such as modeling of soil biological processes that are sensitive to soil water content, particularly at the soil–atmosphere interface.

REFERENCES

Allen, R.G., M.E. Jensen, J.L. Wright, and R.D. Burman. 1989. Operational estimates of reference evapotranspiration. Agron. J. 81:650–662.

Bisal, F., and J. Hsieh. 1966. Influence of moisture on erodibility of soil by wind. Soil Sci. 102(3):143–146.

Brust, K.J., C.H.M. Van Bavel, and G.B. Stirk. 1968. Hydraulic properties of a clay loam soil and the field measurement of water uptake by roots: III. Comparison of field and laboratory data on retention and of measured and calculated conductivities. Soil Sci. Soc. Am. Proc. 32:322–326.

Campbell, G.S. 1974. A simple method for determining unsaturated conductivity from moisture retention data. Soil Sci. 117(6):311–314.

Campbell, G.S. 1985. Soil physics with BASIC: Transport models for soil–plant systems. Elsevier Science Publishers B.V. Amsterdam, The Netherlands.

Chepil, W.S. 1956. Influence of moisture on erodibility of soil by wind. Soil Sci. Soc. Am. Proc. 20:288–292.

Durar, A.A. 1991. Simulation of soil-water dynamics for wind erosion modeling. Ph.D. diss. Kansas State Univ., Manhattan (Diss. Abstr. 91-28491).

Dusek, D.A., T.A. Howell, A.D. Schneider, and K.S. Copeland. 1987. Bushland weighing lysimeter data acquisition systems for evapotranspiration research. ASAE Paper no. 87-2506. ASAE, St. Joseph, MI.

Evett, S.R., and R.J. Lascano. 1993. ENWATBAL.BAS: A mechanistic evapotranspiration model written in compiled BASIC. Agron. J. 85:763–772.

Flerchinger, G.N. 1987. Simultaneous heat and water model of a snow-residue-soil system. Ph.D. diss. Washington State Univ., Pullman (Diss. Abstr. 88-13071).

Fox, D.G. 1981. Judging air quality model performance: A summary of the AMS workshop on dispersion model performance, Woods Hole, MA. 8–11 Sept. 1980. Bull. Am. Meteorol. Soc. 62:599–609.

Hagen, L.J. 1991. A wind erosion prediction system to meet user needs. J. Soil Water Conserv. 46(2):106–111.

Howell, T.A., A.D. Schneider, D.A. Dusek, and T.H. Marek. 1987. Calibration of Bushland weighing lysimeters and scale performance as affected by wind data. ASAE Paper no. 87-2505. ASAE, St. Joseph, MI.

Hillel, D. 1977. Computer simulation of soil-water dynamics: A compendium of recent work. Int. Dev. Res. Ctr., Ottawa, ON.

Idso, S.B., R.D. Jackson, R.J. Reginato, B.A. Kimball, and F.S. Nakayama. 1975. The dependence of bare soil albedo on soil water content. J. Appl. Meteorol. 14:109–113.

Jackson, R.D. 1964. Water vapor diffusion in relatively dry soil: III. Steady-state experiments. Soil Sci. Soc. Am. Proc. 28:467–470.

Jackson, R.D. 1973. Diurnal changes in soil-water content during drying. p. 37–55. *In* R.R. Bruce et al. (ed.) Field soil water regime. SSSA Spec. Publ. 5. SSSA, Madison, WI.

Jackson, R.D., B.A. Kimball, R.J. Reginato, and F.S. Nakayama. 1973. Diurnal soil water evaporation: Time-depth-flux patterns. Soil Sci. Soc. Am. Proc. 37:505–509.

Marek, T.H., A.D. Schneider, T.A. Howell, and L.L. Ebeling. 1988. Design and construction of large weighing monolithic lysimeters. Trans. ASAE 31:477–484.

Mech, S.J. 1955. Wind erosion control in the Columbia Basin. Wash. Agric. Exp. Stn. Circ. 268.

Reginato, R.J. 1975. Sampling soil-water distribution in the surface centimeter of a field soil. Soil Sci. 120(4):292–294.

Robinson, J.M., and K.G. Hubbard. 1990. Soil water assessment model for several crops in the High Plains. Agron. J. 82:1141–1148.

Saxton, K.E., and G.C. Bluhm. 1982. Regional prediction of crop water stress by soil water budgets and climatic demand. Trans. ASAE 25(1):105–110, 115.

Saxton, K.E., H.P. Johnson, and R.H. Shaw. 1974. Modeling evapotranspiration and soil moisture. Trans. ASAE 17(4):673–677.

Schneider, A.D., and T.A. Howell. 1990. Sprinkler efficiency measurement with large weighing lysimeters. p. 69–76. *In* ASAE Publ. 04-90, Visions of the future. Proc. Third National Irrigation Symposium, Phoenix, AZ. 28 Oct–1 Nov. 1990. Am. Soc. Agric. Eng.

Skidmore, E.L. 1979. Surface soil water content. p. 544–551. *In* R.W. Fairbridge and C.W. Finkl, Jr. (ed.) The encyclopedia of soil science. Part 1. Dowden, Hutchinson & Ross, Stroudsburg, PA.

Skidmore, E.L., and L. Dahl. 1978. Surface soil drying: Simulation experiment. Abstracts for commission papers. Int. Soc. Soil Sci., 11th Congr., Edmonton, AB. 19–27 June 1978.

Smith, R.E., and J.R. Williams. 1980. Simulation of the surface water hydrology. p. 13–35. *In* W.G. Knisel (ed.) CREAMS: A field scale model for chemicals, runoff, and erosion from agricultural management systems. USDA Conserv. Res. Rep. 26. USDA, Washington, DC.

Soil Conservation Service. 1972. SCS National Engineering Handbook. Section 4. Hydrology. NEH-Notice 4-102. USDA-SCS, Washington, DC.

Sudar, R.A., K.E. Saxton, and R.G. Spomer. 1981. A predictive model of water stress in corn and soybeans. Trans. ASAE 24(1):97–102.

Taylor, H.M., C.E. Van Doren, C.L. Godfrey, and J.R. Coover. 1963. Soils of the Southwestern Great Plains Field Station. Texas Agric. Exp. Stn. MP-669.

Troeh, F.R., J.A. Hobbs, and R.L. Donahue. 1980. Soil and water con-

servation for productivity and environmental protection. Prentice-Hall, Englewood Cliffs, NJ.
Unger, P.W., and F.B. Pringle. 1981. Pullman soils: Distribution, importance, variability, and management. Texas Agric. Exp. Stn. B-1372.
Van Bavel, C.H.M. 1966. Potential evaporation: The combination concept and its experimental verification. Water Resour. Res. 2(3): 455–467.
Williams, J.R., C.A. Jones, and P.T. Dyke. 1984. A modeling approach to determining the relationship between erosion and soil productivity. Trans. ASAE 27(1):129–144.
Williams, J.R., C.A. Jones, and P.T. Dyke. 1990. The EPIC model. p. 3–92. *In* A.N. Sharpley and J.R. Williams (ed.) EPIC–Erosion/Productivity Impact Calculator: 1. Model documentation. USDA Tech. Bull. 1768. USDA, Washington, DC.
Willmott, C.J. 1981. On the validation of models. Physical Geogr. 2(2):184–194.
Willmott, C.J. 1982. Some comments on the evaluation of model performance. Bull. Am. Meteorol. Soc. 63(11):1309–1313.
Wright, J.L. 1982. New evapotranspiration crop coefficients. J. Irrig. Drain. Div., Am. Soc. Civ. Eng. 108(2):57–74.